[1]L. D. Landau and E. M. Lifshitz, Élektrodinamika sploshnykh sred (Electrodynamics of Continuous Media), Gostekhizdat, M., 1957 (English translation published by Pergamon Press, Oxford, 1960).
[2]Y. B. Kim, C. F. Hempstead and A. R. Strnad, Phys. Rev. **139**, A1163 (1965).
[3]A. F. Andreev, Pis'ma Zh. Eksp. Teor. Fiz. **6**, 836 (1967) [JETP Lett. **6**, 282 (1967)].
[4]V. P. Galaiko, Zh. Eksp. Teor. Fiz. **66**, 379 (1974) [Sov. Phys. JETP **39**, 181 (1974)].
[5]P. W. Anderson, J. Phys. Chem. Solids **11**, 26 (1959).
[6]H. J. Fink, Phys. Lett. **42A**, 465; **34A**, 523 (1973).
[7]I. O. Kulik, Zh. Eksp. Teor. Fiz. **59**, 584 (1970) [Sov. Phys. JETP **32**, 318 (1971)].
[8]L. P. Gor'kov and E. M. Éliashberg, Zh. Eksp. Teor. Fiz. **54**, 612 (1968); **55**, 2430 (1968); **56**, 1297 (1969) [Sov. Phys. JETP **27**, 328 (1968); **28**, 1291 (1969); **29**, 698 (1969)].
[9]V. P. Galaĭkov, Zh. Eksp. Teor. Fiz. **68**, 223 (1975) [Sov. Phys. JETP **41**, 108 (1975)].
[10]L. P. Gor'kov, Pis'ma Zh. Eksp. Teor. Fiz. **11**, 52 (1970) [JETP Lett. **11**, 32 (1970)].
[11]V. P. Galaĭko, Teor. Mat. Fiz. **22**, 375; **23**, 111 (1975) [Theor. Math. Phys. (USSR) **22**; **23**, (1975)].
[12]V. P. Galaĭko, Zh. Eksp. Teor. Fiz. **61**, 382 (1971) [Sov. Phys. JETP **34**, 203 (1972)].
[13]V. P. Galaĭko, V. M. Dmitriev and G. E. Churilov, Fiz. Nizk. Temp. (Low Temperature Physics) **2**, 299 (1976) [Sov. J. Low Temp. **2**, 148 (1976)].
[14]V. P. Galaĭko, V. M. Dmitriev and G. E. Churilov, Pis'ma Zh. Eksp. Teor. Fiz. **18**, 362 (1973) [JETP Lett. **18**, 213 (1973)].
[15]B. D. Josephson, Rev. Mod. Phys. **36**, 216 (1964).
[16]P. W. Anderson and A. H. Dayem, Phys. Rev. Lett. **13**, 195 (1964).
[17]W. J. Skocpol, M. R. Beasley and M. Tinkham, J. Low. Temp. Phys. **16**, 145 (1974).
[18]A. B. Pippard, J. G. Shepherd and D. A. Tindall, Proc. Roy. Soc. **A324**, 17 (1971).
[19]A. A. Abrikosov, Zh. Eksp. Teor. Fiz. **32**, 1442 (1957) [Sov. Phys. JETP **5**, 1174 (1957)].
[20]V. P. Galaĭko, A. V. Svidzinskiĭ and V. A. Slyusarev, Zh. Eksp. Teor. Fiz. **56**, 835 (1969) [Sov. Phys. JETP **29**, 454 (1969)].
[21]S. R. de Groot and P. Mazur, Nonequilibrium Thermodynamics, North-Holland, Amsterdam, 1962 (Russ. transl., Mir, M., 1964).
[22]J. Bardeen, L. N. Cooper and J. R. Schrieffer, Phys. Rev. 108, 1175 (1957).
[23]N. N. Bogolyubov, Zh. Eksp. Teor. Fiz. **34**, 58, 73 (1958) [Sov. Phys. JETP **7**, 41, 51 (1958)].
[24]V. P. Galaĭko, Zh. Eksp. Teor. Fiz. **64**, 1824 (1973) [Sov. Phys. JETP **37**, 922 (1973)].
[25]A. A. Abrikosov and L. P. Gor'kov, Zh. Eksp. Teor. Fiz. **39**, 1781 (1960) [Sov. Phys. JETP **12**, 1243 (1961)].
[26]G. E. Churilov, V. M. Dmitriev and A. P. Beakorsyĭ, Pis'ma Zh. Eksp. Teor. Fiz. 10, 231 (1969) [JETP Lett. 10, 146 (1969)].
[27]J. M. Smith and M. W. P. Strandberg, J. Appl. Phys. **44**, 2365 (1973).
[28]J. D. Meyer, Appl. Phys. **2**, 303 (1973).

Translated by P. J. Shepherd

Electron-phonon interaction spectrum in copper

I. K. Yanson and Yu. N. Shalov

Physico-technical Institute of Low Temperatures, Ukrainian Academy of Sciences
(Submitted December 24, 1975)
Zh. Eksp. Teor. Fiz. **71**, 286–299 (July 1976)

The nonlinear current-voltage characteristics of microscopic copper point junctions are investigated at low temperatures ($\lesssim 4.2$°K). The electron-phonon interaction function $g(\omega)=\alpha^2(\omega)F(\omega)$ is reconstructed from the voltage dependence of the second derivative of the current-voltage characteristics. It is found that $g(\omega)$ differs appreciably from the phonon state density $F(\omega)$, owing to the strong mean square matrix element dependence of the electron-phonon interaction energy α^2. New effects are observed at low energies corresponding to large mean free paths. These include oscillations of the second derivative and a minimum of conductivity at $V=0$. These effects are apparently due to quantum size effects and to nonequilibrium occupation of the electron states near the Fermi level.

PACS numbers: 71.85.Ce

1. INTRODUCTION

One of us[1] has proposed a new method of investigating electron-phonon interactions (EPI) in normal metals. It has turned out that at $T\approx 0$ the second derivatives of the current-voltage characteristics of point junctions are directly proportional to a function of the EPI

$$g(\omega)=\alpha^2(\omega)F(\omega), \tag{1}$$

equal to the product of the square of the matrix element of the EPI, averaged over the Fermi surface, and to the density of the phonon states.[2] This was experimentally demonstrated for point junctions with dimensions on the order of several dozens angstroms made of metals such as Pb, Sn,[1] and In,[3] for which the function $g(\omega)$ is known from tunnel measurements in the superconducting state.[4]

For many metals, however, an investigation of nonlinear effects in point junctions is the only way of determining the function $g(\omega)$ over the entire energy interval. This pertains primarily to noble metals with weak EPI, such as Cu, Ag, and Au. The present paper is devoted to an experimental investigation of the spectrum of the EPI in copper. The function $g(\omega)$ obtained by us differs

significantly from the known density of the phonon states $F(\omega)$,[5] thus indicating an appreciable energy dependence of the mean squared matrix element of the EPI. In addition, new effects have been observed at low energies corresponding to large electron-phonon free path lengths. These include oscillations of the second derivative of the current-voltage characteristic and a minimum of the conductivity at $V=0$. These effects were not observed in the previously investigated metals with stronger EPI (Pb, Sn, In), and are apparently typical of metals with weak EPI.

The function $g(\omega)$ obtained in the present paper can be used to calculate many copper properties, governed by the interaction of electrons with phonons. In particular, it can be used to calculate the temperature dependences of the electric conductivity and of the electronic thermal conductivity in a wide range of temperatures.

2. THE MODEL

We consider the model proposed by Sharvin,[6] in which the point junction constitutes a hole of diameter d_0 in an infinitesimally thin partition. The resistance of such a junction, which joins two identical metals, is approximately equal to[1]

$$R \approx R_0 (1 + d/l), \tag{2}$$

where $R_0 = \rho l / d_0^2$ according to Sharvin, and ρ is the resistivity. For copper $\rho l = 0.53 \cdot 10^{-11}$ Ω-cm^2.[7] The mean free path l is governed by the scattering of the electrons by the impurities (l_{imp}) and by the phonons ($l_{e\text{-}ph}$):

$$1/l = 1/l_{imp} + 1/l_{e\text{-}ph}, \tag{3}$$

the last term being dependent on the electron energy, and consequently on the voltage V applied to the junction. If the impurity mean free path is different in the two electrodes, then we must substitute in formula (3) the mean value

$$\langle 1/l_{imp} \rangle = \frac{1}{2} (1/l_{imp\,1} + 1/l_{imp\,2}).$$

In real contacts, the conducting channel joining both metals can have a finite length L. In this case, to determine the effective junction diameter we can use an interpolation formula

$$R \approx \frac{\rho l}{d^2} \left(1 + \frac{L}{d} + \frac{d}{l}\right), \tag{4}$$

which in the limit $L \gg d$ gives the resistance of a thin metallic filament with average mean free path equal to the filament diameter d.

As shown earlier,[1] at low temperatures the second derivative of the current-voltage characteristic is directly proportional to the function $g(\omega)$:

$$\frac{dR_D}{dV} = \frac{2\pi d_0 R_0}{\hbar v_0} \int_0^\infty g(\omega)\, \Phi\left(\frac{\hbar\omega - eV}{kT}\right) d\omega$$

and as $T \to 0$ we have

$$\frac{dR_D}{dV} \approx \frac{2\pi d_0 R_0}{\hbar v_0} g(eV), \tag{5}$$

where $R_D = dV/dI$ is the differential resistance, v_0 is the Fermi velocity, and

$$\Phi(z) = e^{-z} \frac{(z-2) + (z+2)e^{-z}}{(1-e^{-z})^3} \tag{6}$$

is a bell-shaped function, that differs from zero in an interval on the order of several kT. As is well known,[8] this function leads to a smearing of the δ-peak into a curve with half-width $5.44kT$.

Formula (5) is valid if the effective temperature of the electron T^e_{eff} is much smaller than the maximum energy eV of the "hot" electrons. Hence we have in order of magnitude[1]

$$kT^e_{eff} \approx eV\, d/l, \tag{7}$$

The condition formulated above is equivalent to the inequality

$$d/l \ll 1, \tag{8}$$

which holds for high-resistance junctions ($R > 10$ Ω).

The EPI junction can no longer be directly measured if $d/l \approx 1$ and $kT^e_{eff} \approx eV$. Thus, the main experimental difficulty lies in the production of point junctions of sufficiently small diameter, since at $eV > \hbar\omega_{max}$ (ω_{max} is the maximum frequency of the phonon spectrum) the value of l cannot be made to exceed $(l_{e\text{-}ph})_{min} = 10^{-5} - 10^{-6}$ cm. In the limit $d/l \ll 1$, the observed nonlinear characteristics should not depend significantly on the microstructure of the junction, since they are determined by the scattering of the electrons by the phonons at a relatively large distance from the junction opening.

3. SAMPLE PREPARATION AND EXPERIMENTAL TECHNIQUE

The construction of the sample is shown in Fig. 1. Copper films several thousand Å thick were evaporated in a vacuum of ~ 10^{-6} Torr on substrates of crystalline quartz or glass at room temperature. The metallic films were separated by two insulator layers of silicon monoxide, one of which (with holes) had a thickness

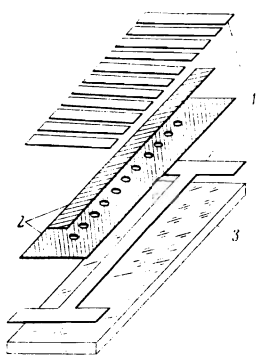

FIG. 1. Sample structure. The sequence of depositing the films in vacuum corresponds to their relative arrangement in the figure. 1—Copper films, 2—SiO films, 3—substrate.

TABLE I.

Junction number	R_0, Ω	ν	l_{imp}, Å	L, Å	d_0, Å	d, Å	d_0/l	d/l	g_{max}	Method of short-circuiting
1	122	0.06	600	420	21	60	0.056	0.16	0.1	–
2	66.2	0.2	600	290	28	66	0.075	0.17	0.116	–
3	61.6	0	600	430	29	76	0.078	0.20	0.145	–
4	49.5	0.14	700	270	33	72	0.08	0.175	0.13	–
5	15.7	0.22	600	290	58	113	0.15	0.3	0.113	Puncture + breakdown
6	13.8	0.15	600	430	62	131	0.16	0.35	0.06	–
7	13.7	0.19	600	290	62	119	0.16	0.32	0.051	Puncture
8	18	0.39	600	290	54	107	0.14	0.28	0.076	Puncture
9	9.5	0.49	600	430	75	151	0.2	0.4	0.064	Breakdown
10	8.4	0.36	600	290	79	143	0.21	0.38	0.041	Puncture
11	6.2	0.55	500	150	92	141	0.28	0.42	0.024	–
12	3.1	0.34	1050	200	131	195	0.26	0.38	0.031	–
13	3.0	0.7	500	150	133	195	0.4	0.58	0.02	–
14	1.04	0.86	480	200	226	342	0.7	1.05	0.022	–
15	0.81	1	480	200	256	389	0.78	1.2	0.01	–

larger than 1000 Å and served to screen the edges, while the other—the thin layer—was used to produce a working area of 2 mm diameter at the intersection center. The width of the lower and upper copper films was 3.5 mm, and their lengths were 70 and 25 mm respectively. The thicknesses of the metallic and dielectric films were monitored with the aid of a quartz pickup during the course of condensation. In the finished structure, the thickness of the metallic films was measured with the aid of a MII-4 microinterferometer, and the thickness L of the barrier layer was calculated from the results of measurements of the capacitance of one or two non-shorted junctions at helium temperature. The dielectric-layer thickness determined in this manner in the working region agreed well with that specified in the course of evaporation, if we put $\varepsilon(SiO) = 3$.

An important parameter is the (effective) impurity mean free path in the films, determined from the formula

$$l_{imp} = 310(R_{300}/R_{4.2} - 1)\,[\text{Å}], \qquad (9)$$

where 310 Å is the electron-phonon mean free path in pure copper at 300 °K, while $R_{300}/R_{4.2}$ is the ratio of the resistances at 300 and at 4.2 °K. It should be noted, however, that formula (9) yields the average value of l_{imp} in the film. In the immediate vicinity of the junction opening, l_{imp} can be either larger of smaller than its mean value, depending on the local structure of the film, on the method of producing the short circuit, etc. This introduces an appreciable uncertainty in the estimate of the effective diameter of the junction with the aid of relations (2) and (4).

It was possible to produce up to 11 junctions on a single structure (Fig. 1). The point junctions were produced: a) by spontaneous short circuit in the course of preparation or subsequent mounting of the sample in the cryostat; b) by applying, with a sharply-pointed steel needle, a local pressure at the center of the working region, thus cracking of the dielectric layer and causing a short circuit at room temperature (puncture); c) as a result of electric breakdown in liquid helium. The junctions, which had approximately the same resistances but were prepared by different methods, had identical characteristics within the scatter characteristic of junctions made by one and the same method.

We selected for the measurements junctions with metallic conductivity. The resistances of such contacts increased with increasing both voltage and temperature. Altogether we investigated the current-voltage characteristics of several hundred junctions. Out of these, several dozen were of relatively high resistance and satisfied the condition (8). The parameters of 15 typical representatives of all types of junctions are listed in Table I.

The effective junction diameter was determined by Sharvin's formula without allowance for the channel length $d_0 = [\rho l/R_0]^{1/2}$ and by formula (4) with correction for the maximum possible junction length L, approximately equal to the thickness of the insulator layer in the working region. Sharvin's value of d_0 was assumed to be more probable, since the insulator layer obtained by deposition in vacuum was apparently inhomogeneous and the short circuit was produced in the place where its thickness was minimal. Obviously, the determination of the effective diameter d and the associated possibility of quantitatively determining the EPI function $g(\omega)$ are arbitrary to a considerable degree, since the model depends essentially on the geometry of the junction, on the purity of the metal, etc. It is all the more important to emphasize that the functional dependence of the second derivative is proportional to $g(\omega)$ and does not depend on these parameters if the condition (8) is satisfied.

Small nonlinearities of the current-voltage characteristics were measured by a four-contact method with direct and alternating current. In the former case we measured the dependence of the static resistance $R_{st} = V/I$ on the voltage across the junction with the aid of the bridge circuit shown in the insert of Fig. 2. The advantage of this circuit lies in its simplicity and reliability. We used in it the same instruments that were used to plot the current-voltage characteristics, but the dc amplifier was switched over to more sensitive limits, which determined in fact the sensitivity of the circuit. This quantity can be easily reduced to 0.01% or less of the initial sample resistance.

In the case of alternating-current measurements we used the standard procedures for separating, amplifying, and synchronously detecting the first and second harmonics of the modulating signal on the sample.[9] In this case one measures the differential resistance $R_D = dV/dI$ and its derivative with respect to voltage on the sample. This technique is used successfully in the investigation of EPI in superconductors[10] and in the

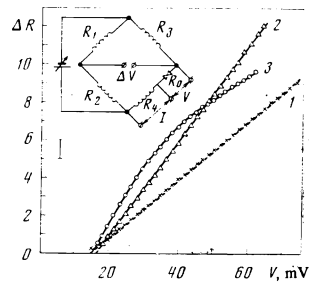

FIG. 2. Static resistance $R_L = R_0 + \Delta R(V)$ of point junctions vs the voltage. Curves 1, 2, and 3 pertain to junctions 12, 9, and 4 from the table. Each ordinate division corresponds respectively to 10.5, 16, and 11 mΩ. The temperature is $T = 4.2$ °K, The insert shows the bridge circuit used to measure small nonlinearities.

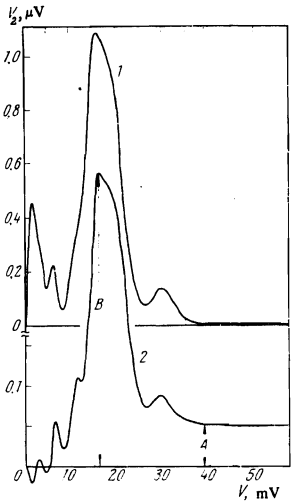

FIG. 3. Dependence of the second-harmonic voltage of the modulating signal on the sample for junctions Nos. 3 and 4 (see the table) with small $\gamma = A/B$. The effective values of the modulating voltage are 0.8 and 0.5 mV, while the temperatures are 4.2 and 1.6 °K for curves 1 and 2, respectively.

spectroscopy of various excitations in a barrier layer by the method of the inelastic tunnel effect.[11] The sensitivity of the second-harmonic channel was ~ 10^{-8} V at a modulation frequency 464 Hz.

4. MEASUREMENT RESULTS

1. Dependence of static resistance on the voltage.

Since the changes of the static resistance are small

$$R_{st} = R_0 + \Delta R(V), \quad \Delta R \ll R_0,$$

it can be easily shown that in the case $R_{st} \ll R_3$ (see the insert in Fig. 2) a simple relation exists between ΔR and the bridge-unbalance voltage ΔV:

$$\Delta V/I \approx \Delta R. \tag{10}$$

Therefore the function $\Delta R(V)$ of interest to us was obtained from two curves, $V(I)$ and $\Delta V(I)$, automatically plotted with an x-y recorder.

Up to a voltage $V \approx 17$ mV, the current-voltage characteristic is linear and $\Delta R = 0$. The corresponding experimental points were left out of Fig. 2 so as not to clutter up the figure. At $eV > 17$ mV, for most junctions with resistance $R_0 < 10$ Ω, the increase of ΔR with voltage is linear (curves 1 and 2), and the intercept of the $\Delta R(V)$ curve with the abscissa axis does not depend on the junction resistance R_0 and is a characteristic of the investigated metal.[12] This voltage (≈ 17 mV for copper) is an important characteristic of the EPI spectrum of the investigated metal.

On the other hand, high-resistance junctions ($R_0 > 10$ Ω) have nonlinear $\Delta R(V)$ dependences (curve 3). We note that within certain limits the described characteristics do not depend on the change in the heat outflow from the sample,[1,2] thus indicating that the heating of the lattice plays no role. It is seen from Fig. 2 that the relative change of the resistance increases with decreasing resistance R_0 and ranges from 0.2% for high-resistance samples to 3% and more for low-resistance junctions. It is interesting to note that the absolute increment of the resistance is of the same order for all samples, despite the fact that their resistances R_0 differ by more than one order. The additional increase of the resistance, observed for very low-resistance junctions ($R_0 < 1$ Ω), is due to heating of the lattice, which cannot be neglected.

2. Dependence of the second derivatives of the current-voltage characteristics on the voltage

For junctions with small dimensions, the dependences of the second derivatives of the current-voltage characteristics on the voltage are proportional to the EPI spectrum in the investigated metal (formula (5)). The $R_{st}(V)$ dependences cited in the preceding section can be obtained for any junction by integrating the second derivatives. Therefore the automatically plotted experimental second-harmonic voltages V_2 of the modulating signal against the junction voltage V constitute the basic initial data used to reconstruct the function $g(\omega)$.

The following relations hold for a measuring circuit with a current source:

$$\frac{d^2V}{dI^2} = 4\frac{V_2}{(i_1)^2}, \quad \frac{d}{dV}\left(\frac{dV}{dI}\right) = \frac{d^2V}{dI^2}\frac{dI}{dV} = 4\frac{V_2}{V_1 i_1} \approx \text{const} \cdot V_2, \tag{11}$$

where i_1 is the amplitude of the modulating current, and V_1 is the first-harmonic voltage across the sample. The last relation in (11) is satisfied with good accuracy, since the variation of V_1 in the entire interval of voltage does not exceed several percent. Thus, the second-harmonic voltage V_2 is proportional to the second derivatives of the current-voltage characteristics d^2V/dI^2 and $(d/dV)(dV/dI)$, which differ only by a constant factor.

Since the structure of the microscopic point junctions remains unknown and depends considerably on the particular case, the reproducibility of measured characteristics of different samples becomes particularly significant and offers evidence that the investigated properties are independent of the structure of the junction. The reproducibility of the $V_2(V)$ characteristics can be assessed from Figs. 3–5, which show the results for samples with different resistances. All the $V_2(V)$ characteristics have a maximum at a voltage $V \approx 17$ mV. An important parameter is the background level at voltages higher than ≈ 35 mV, corresponding to the end of the phonon spectrum of the copper. The relative level of the background can be quantitatively described with the aid of the empirical parameter $\gamma = A/B$, the definition of which is clear from Fig. 3 (curve 2). The physical meaning of the parameter γ will be discussed later on.

Figure 3 shows the characteristics of junctions with small values of γ and with resistances on the order of 100 Ω, Fig. 4 shows junctions with intermediate γ and resistances ~ 10 Ω, and Fig. 5—with large γ and resistances ~ 1 Ω. If we disregard the initial oscillatory section, then all spectra have obvious common properties: a principal maximum at $V = 17$ mV and a small maximum at $V = 30$ mV. The latter, however, does not appear in low-resistance junctions with a large background level (Fig. 5). The asymmetrical shape of the principal maximum is well duplicated in different samples, and its half-width does not depend on the temperature in the interval 1.6–4.2 °K or on the amplitude of the modulation voltage, provided the latter is small enough ($V_1 < 1$ mV).

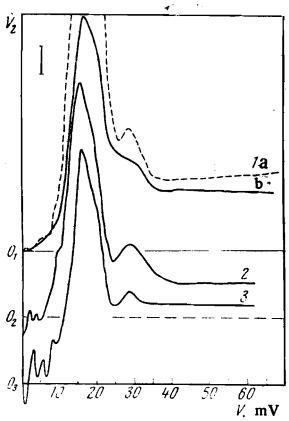

FIG. 4. Dependence of the second-harmonic voltage of the modulating signal on the constant voltage on the same for junctions Nos. 5, 6, 12—curves 1b, 2, 3. The effective values of the modulating voltages are 0.5 mV, the temperatures are 4.2, 4.2, 1.6, and 1.6 °K, each division of the V_2 scale (indicated in the figure in the upper left corner) corresponds to $8.5, 3.1, 4.1$, and 5.9×10^{-8} V for curves 1a, 1b, 2, and 3, respectively.

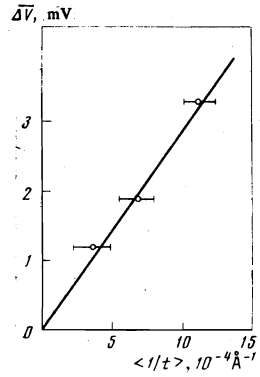

FIG. 6. Dependence of the average period of the oscillations on the reciprocal thickness of the copper films: $\langle 1/t\rangle = \frac{1}{2}(1/t_1 + 1/t_2)$, where t_1 and t_2 are the thicknesses of the upper and lower films.

If we compare the parameter γ and the ratio d/l, which determines the heating of the electron gas (formula (7)), then we can note a correlation between d/l and the value of γ minimal for the given d/l (insert in Fig. 5). The fact that such a correlation is observed precisely for γ_{min} is not surprising, since films having equal averaged values of l_{imp} can have impurity and defect concentrations that are larger in the region of the junction, as a result of electric or mechanical damage to the dielectric layer during the short circuiting. This leads to a local decrease of l_{imp} and to an increase of γ, whereas γ_{min} corresponds to relatively "pure" junctions, for which the model is valid. Thus, the approximate correspondence between γ_{min} and d/l means that the empirical parameter γ, roughly speaking, corresponds to the ratio of the effective temperature of the electron gas to the maximum energy eV of the "hot" electrons (formula (7)). Consequently, only junctions with sufficiently small values of γ are suitable for the study of the EPI spectrum.

The $V_2(V)$ characteristics of junctions with large γ (Fig. 5) are different at $eV > \hbar\omega_{max}$, depending on the extent to which the lattice heating plays a role. In the case of good heat outflow from the lattice, $V_2(V)$ is approximately constant or increases very weakly with increasing V, and does not depend on the change of the heat removal within certain limits. On the other hand, if the heating of the lattice cannot be neglected, then $V_2(V)$ increases noticeably with increasing V (curves 3, 1, and 4 in Fig. 5), and this increase depends significantly either on the change of the substrate material (glass–crystalline quartz), or on the transition through the λ point in the liquid helium. It follows from the foregoing that the characteristics shown in Figs. 3 and 4 correspond to negligibly small heating of the lattice in comparison with the heating of the electron gas, which is also small for high-resistance junctions (small γ).

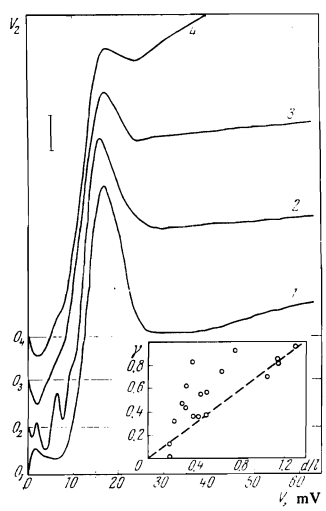

FIG. 5. The $V_2(V)$ characteristics for samples No. 9, 13, 14, and 15. Each division on the y axis corresponds to 4.6, 3.6, 4.6, and 2.6×10^{-8}V, at $V_1 = 0.7$ mV, for curves 1, 2, 3, and 4, respectively. $T = 4.2$ °K. The insert shows a plot of γ (see Fig. 3, curve 2) against the ratio of the junction diameter to the mean free path at $eV = 35$ meV.

3. Singularities of the second derivative of the current-voltage characteristics in the region of low voltages

The greater part of the $V_2(V)$ characteristics exhibited singularities, with different relative magnitudes, in the region of low voltages (< 17 mV). These singularities are observed on practically all the characteristics shown in Figs. 3–5, with the possible exception of curve 1b of Fig. 4. But even in the latter case they can be noticed on the characteristic of the same junction, plotted up to the instant when its resistance was decreased by a factor of two as a result of electric breakdown (curve 1a). The observed singularities can be divided into two types, which are typical of high-resistance and low-resistance junctions.

We include in the first type of singularities the oscillations of $V_2(V)$, which can be noted on many of the characteristics shown in Figs. 3–5. These oscillations hinder the observation of the EPI spectrum, but their study is nevertheless of independent interest. The following properties of the oscillations have been established experimentally:

1) The period of the oscillations depends on the film thickness. This dependence plays a crucial role in the explanation of the mechanism whereby the oscillations are produced. Figure 6 shows preliminary data on the results of the measurements on three samples having approximately the same thickness of the two copper films. The error in the thickness determination was ± 200 Å.

2) The amplitude of the oscillations decreases as $eV \to \hbar\omega_{max}$. No oscillations are observed at $eV > \hbar\omega_{max} = 35$ mV.

3) The $V_2(V)$ plots of junctions having the same structure differ only in amplitude and shape, but not in the

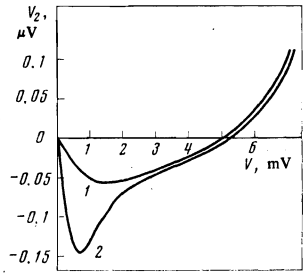

FIG. 7. Temperature dependence of the minimum of the $V_2(V)$ characteristic near $V=0$. Curves 1 and 2 correspond to the temperatures 4.2 and 1.6 °K; $R_0=0.4\ \Omega$, $V_1=1$ mV.

positions of the singularities relative to the V axis. Consequently, the period of the oscillations does not depend on the junction resistance and on its detailed structure.

4) The amplitude of the oscillations is smaller the smaller the junction resistance and the larger its effective radius. This property can be traced also for junctions whose characteristics are shown in Figs. 3–5.

Properties 3) and 4) are well supported, both by a study of the characteristics of different junctions belonging to one and the same structure, and by studies of one and the same contact whose resistance was varied many times in such a way that it decreased as a result of the electric breakdown by more than one order of magnitude. A study of the $V_2(V)$ oscillations during each intermediate stage of the short-circuiting has shown that the shape of the curve remains unchanged, and only the amplitude decreases.

5) In contrast to the principal part of the $V_2(V)$ characteristic, which is always symmetrical with respect to reversal of the polarity of the applied voltage, the $V_2(V)$ plots exhibit oscillations, both symmetrical and asymmetrical, with respect to the origin.

6) When the temperature is changed from 1.5 to 10 °K, the positions of the oscillating singularities relative to the V axis remain unchanged, but their amplitude decreases. The character of the cooling (by gaseous, normal-liquid, or superfluid helium) does not affect the observed singularities.

The second type of singularity at low voltages is typical of low-resistance junctions and corresponds to a minimum in the region near $V=0$, where V_2 becomes negative. This minimum is symmetrical about the origin and corresponds to a maximum of dV/dI at $V=0$. The effect is all the more noticeable the smaller the junction resistance, and can therefore be investigated separately from the oscillations (curves 3 and 4 in Fig. 5). Figure 7 shows the initial section of the characteristic $V_2(V)$ for one of the low-resistance junctions at two temperatures. The position of the minimum shifts towards lower V with decreasing temperature, and its intensity increases.

5. DISCUSSION OF EXPERIMENTAL RESULTS

1. Linear dependence of the static resistance on the voltage

A linear dependence of R_{st} on the voltage is typical of junctions with $\gamma \sim 1$. In this case the effective temperature of the electron gas is of the order of eV, and the model considered in Sec. 2 cannot be used. At sufficiently good heat outflow from the lattice, however, the temperature of the latter remains appreciably lower than the temperature of the electron gas, so that the theoretical results of Kaganov, Lifshitz, and Tanatarov[22] can be used. According to this theory, the energy transfered by the electrons to the lattice per unit time and in a unit volume is in our case

$$w=\pi^2 m s^2 n_0/6\tau(T^e_{\text{eff}}), \tag{12}$$

where s is the speed of sound, n_0 is the electron density, $\tau(T^e_{\text{eff}})$ is the free-path time of the electrons under the condition that the lattice temperature coincides with the effective temperature of the electron gas. Inasmuch as at $eV>\hbar\omega_{\max}$ we have $kT^e_{\text{eff}}=\text{const}\cdot eV>\hbar\omega_{\max}$, it follows that $\tau\propto 1/eV$ and $w\propto eV$. Consequently, the voltage-dependent part of the resistance $\Delta R(V)$, due to the scattering of the electrons by phonons, is proportional to eV at $eV>\hbar\omega_{\max}$.

The experimentally obtained linear dependence sets in somewhat earlier than at $eV=\hbar\omega_{\max}=35$ meV, namely in the vicinity of the principal maximum of the EPI spectrum at $V=17$ mV. This discrepancy is apparently due to the simplifications incorporated in the theory, in which it is assumed that the phonon and electron distributions are described by the Bose and Fermi equilibrium distribution functions, and that the lattice vibrations have a Debye spectrum.

2. Reconstruction of the spectrum of the electron-phonon interaction in copper.

To reconstruct the EPI spectrum we used the initial section of the $V_2(V)$ characteristic, which contains no singularities (curve 1b of Fig. 4), and the remaining part (with two maxima) of the characteristic with $\gamma=0$ (curve 1 of Fig. 3). The joining point was chosen to be $V=11$ mV, the subsequent behavior of the characteristics up to $V\approx 20$ mV is practically the same, and the difference comes into play only at $V>20$ mV, when the influence of the heating of the electron gas becomes significant. Replacement of the initial section of the characteristic of the high-resistance junction No. 3 by the characteristic of the lower-resistance junction No. 5 (see Table I) does not lead to deviations from the model, for despite the corresponding increase of d_0 (or d), the ratio d_0/l (or d/l) remains as before much smaller than unity, so that at small eV the electron-phonon mean free path is large.

The function $g(\omega)$ constructed in this manner for copper, and constituting the principal result of the present study, is shown in Fig. 8b (curve 1). As expected, its initial section is quadratic in eV, therefore the results of dividing $g(eV)$ by eV (curve 2) yields a straight line at small eV.

The ordinate axis was calibrated in accordance with the known value[13] of the EPI parameter λ for copper:

$$\lambda=2\int_0^\infty \frac{g(\omega)}{\omega}d\omega=0.14\pm0.03. \tag{13}$$

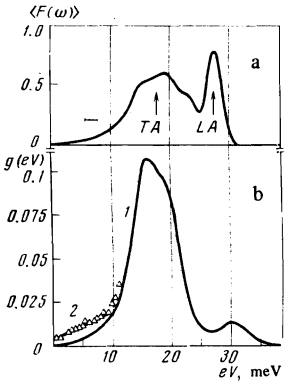

FIG. 8. a) Phonon spectrum of copper, averaged in an interval ±1 mV near each point, for from the data of[5]. The total averaging interval is shown in the figure by the horizontal segment. b) Spectrum of electron-phonon interaction in copper (curve 1). Curve 2 is the result of dividing $g(eV)$ by eV.

From this we obtain for the maximum value of $g(eV)$

$$g_{max}=0.107\pm0.023. \tag{13a}$$

The g scale can be calibrated by using relation (5). However, as seen from the table, the values of g_{max} obtained in this manner change significantly from sample to sample, decreasing on the average much more noticeably with increasing $\gamma > 0.4$. Recognizing that the assumed model pertains to $\gamma \ll 1$ and assuming that the scatter of the values of g_{max} is due to random factors, we determine the average value of g_{max} and the standard deviation first only from the data for high-resistance junctions (Nos. 1–4 in the table):

$$g_{max}=0.12\pm0.01, \tag{14}$$

and then from the results for the junctions Nos. 1–7 with $\gamma \lesssim 0.2$:

$$g_{max}=0.10\pm0.013. \tag{15}$$

All three values (13a), (14), and (15) are in surprisingly good agreement. This agreement, however, must not be regarded as too significant, since analogous calculations for other metals lead to agreement between the values of g, calculated by formula (5), and the known values on tunnel data in the superconducting state only in order of magnitude, reflecting only qualitatively the growth of g with increasing EPI strength.

Since the temperature at which the EPI spectrum is measured is much lower than the Debye temperature, the spectrum obtained at $T=4.2\,^\circ$K differs little from the spectrum at $T=0$. Indeed, the $V_2(V)$ characteristics do not change noticeably though when the temperature is lowered from 4.6 to 1.6 °K.

The electron-phonon collision frequency integrated over the Fermi surface is an integral of the function $g(\omega)$

$$\frac{1}{\tau_{e\text{-}ph}}=\frac{2\pi}{\hbar}\int_0^{eV} g(\omega)\,d\omega. \tag{16}$$

Using the function $g(\omega)$ obtained by us, we can plot $1/\tau_{e\text{-}ph}$ against eV for copper (Fig. 9). The minimum mean free path in copper, averaged over the Fermi surface, is $\approx 10^{-5}$ cm (at $v_0 = 10^8$ cm/sec).

The function $g(\omega)$ is usually compared with the density of the phonon states $F(\omega)$, and the agreement between the two is good, meaning that α^2 depends little on the energy. Such an agreement was observed for metals with three and more electrons per atom (Pb, Sn, In, and others), the Fermi surface of which greatly exceeds the dimensions of the first Brillouin zone. The density $F(\omega)$ of the phonon states for copper is known from neutron-diffraction data[5] and constitutes two maxima, a broad one at $eV_{TA}=14$–21 meV, due to transverse phonons, and a narrow one at $eV_{LA}=27$ meV, corresponding to longitudinal acoustic phonons. After averaging $F(\omega)$ near each point in an interval ±1 mV, corresponding to the thermal smearing of the Fermi step 5.44 kT at 4.2 °K in our experiments, this dependence (Fig. 8a) should be compared with the EPI spectrum (Fig. 8b).

The position of the maximum due to the transverse phonons (TA maximum) is the same on both spectra. The maximum due to the longitudinal phonons (LA maximum) is shifted on the EPI spectrum towards higher energies (by approximately 2 meV). On the EPI spectrum the intensity of the LA maximum is smaller by one order of magnitude than that of the TA maximum. Consequently $\alpha^2_{LA}(\omega) \ll \alpha^2_{TA}(\omega)$. The ratio of the intensities of the TA and LA maxima in the EPI spectrum is regarded in[15] as a rough measure of the fraction of the Umklapp processes in the entire aggregate of the electron-phonon scattering processes. Consequently it can be concluded that in copper the Umklapp processes, which involve transverse phonons and scattering of the electrons, play the principal role. A similar conclusion follows from the experimental[16,17] and theoretical[18,19] studies of the dependence of the frequency of the scattering of Fermi electrons by phonons on the position of a point on the Fermi surface.

3. Quantum size effect and effect of blocking of the electronic states at small V.

The linear dependence of the period of the oscillations on the reciprocal film thickness (Fig. 6) suggests that the probable cause of their appearance is the quantum size effect. Since the period of the oscillations is in this case

$$\Delta(eV)=\hbar v_0\pi/t, \tag{17}$$

it follows from the slope of the straight line in Fig. 6 we can determine v_0, which turns out to be equal 0.14×10^8 cm/sec. This is several times smaller than the Fermi velocity of the electrons in copper.[20] The rea-

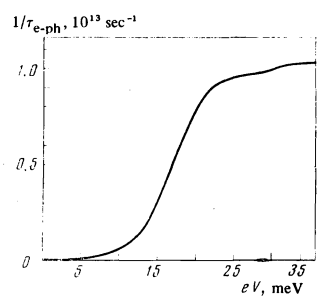

FIG. 9. Energy dependence of the electron-phonon collision frequency averaged over the Fermi surface in copper at $T \approx 0$.

son for this discrepancy is not clear.

A qualitative explanation of the minimum near $V = 0$ (Fig. 7) can be obtained by comparing the $V_2(V)$ characteristics of point junctions with analogous characteristics of tunnel junctions, for which effects of nonequilibrium distribution of the electrons in energy are significant.[21] At sufficiently large injection velocity of the "hot" electrons, which corresponds to low-resistance contacts, the states near the Fermi level turn out to be populated with a noticeable excess as against the equilibrium distribution. This decreases somewhat the conductivity near $V = 0$ (the so called effect of blocking of states[21]).

The range of voltages at which the minimum of $V_2(V)$ is observed, and the dependence of this minimum on the V axis and of its height on the temperature for point junctions of copper agree qualitatively well with the results of tunnel measurements on aluminum,[21] which also has a weak EPI.

6. CONCLUSION

We have shown that an investigation of the nonlinear effects in the electric conductivity of point junctions makes it possible to determine the function $g(\omega)$ not only for metals with strong EPI, but also for well-conducting metals with weak EPI, a typical representative of which is copper. The nonlinearity for copper is not much smaller than in the case of such metals as lead, tin, or indium, and amounts from several tenths of a percent to several percent of the initial value of the junction resistance. With the aid of modern tunnel-spectroscopy techniques, such nonlinearities can be easily detected and can be measured with high accuracy.

It is obvious that the procedure described in this paper for determining the function $g(\omega)$ can be easily generalized to include other noble metals (Ag, Au). This was demonstrated experimentally earlier,[1] with a silver junction having a relatively large γ as an example (Fig. 7b in[1]). Further advances in the method should therefore follow the path of developing an experimental procedure for producing high-resistance small-γ junctions of silver, gold or other metals.

It was observed in the present study that metals with weak EPI are characterized by the appearance of new singularities on the second derivatives of the current-voltage characteristics, the study of which is of independent interest. These include non-equilibrium effects of occupation of the electron states, and the quantum size effects.

From the experimental point of view, an extensive application of the method developed by us for the investigation of EPI in normal metals is strongly hindered by the lack of methods for controlled production of pure junctions with microscopic dimensions (on the order of several dozen angstroms). On the other hand, the lack of a rigorous theory of nonlinear effects in such junctions also hinders greatly the progress in this field.

[1] I. K. Yanson, Zh. Eksp. Teor. Fiz. 66, 1035 (1974) [Sov. Phys. JETP 39, 506 (1974)].
[2] N. V. Zavaritskiĭ, Usp. Fiz. Nauk 108, 241 (1972) [Sov. Phys. Usp. 15, 608 (1973)].
[3] I. K. Yanson, Fiz. Tverd. Tela (Leningrad) 16, 3595 (1974) [Sov. Phys. Solid State 16, 2337 (1975)].
[4] J. M. Rowell, W. L. McMillan, and R. C. Dynes, Tabulation of the Electron-Phonon Interaction in Superconducting Metals and Alloys, p. 1 (preprint).
[5] J. W. Lynn, H. G. Smith, and R. M. Nicklow, Phys. Rev. B8, 3493 (1973).
[6] Yu. V. Sharkin, Zh. Eksp. Teor. Fiz. 48, 984 (1965) [Sov. Phys. JETP 21, 655 (1965)].
[7] J. J. Gniewek, J. C. Moulder, and R. H. Kropschot, Tr. X Mezhdunarodnoĭ konferentsii po fizike nizkikh temperatur (Proc. Tenth Internat. Conf. on Low-Temperature Physics) 3, Moscow, VINITI, 1967, p. 366.
[8] R. C. Jacklevic and J. Lambe, Phys. Rev. 165, 821 (1968).
[9] N. P. Mikhin and I. K. Yanson, Fizika kondensirovannogo sostoyaniya (Physics of the Condensed State), No. 29, Khar'kov, FTINT Akad. Nauk Ukr. SSR, 1973.
[10] W. L. McMillan and J. M. Rowell, Superconductivity, ed. R. D. Parks, 1, New York, 1969, p. 561.
[11] J. Lambe and R. C. Jaklevic, in: Tunneling Phenomena in Solids, E. Burstein and S. Lundquist, eds. Plenum, 1969 [Russ. transl., Mir, 1973, p. 223].
[12] I. K. Yanson, Dissertation, FTINT Akad. Nauk Ukr. SSSR, Char'kov, 1975.
[13] G. Grimvall, Phys. Kondens. Mater. 11, 279 (1970).
[14] J. M. Rowell and R. C. Dynes, in: Phonons, ed. M. A. Fusimovici, 1971, p. 150.
[15] R. C. Dynes, J. P. Carbotte, and D. W. Taylor, Phys. Rev. 178, 713 (1968).
[16] V. F. Gantmakher, Rep. Prog. Phys. 37, 317 (1974).
[17] R. E. Doezema and J. F. Koch, Phys. Rev. B6, 2071 (1972).
[18] D. Nowak, *ibid.*, 3691.
[19] S. G. Das, Phys. Rev. B7, 2238 (1973).
[20] R. E. Doezeme and J. F. Koch, Phys. Rev. B5, 3866 (1972).
[21] P. N. Trofimenkoff, H. J. Kreuzer, W. J. Wattamaniuk, and J. G. Adler, Phys. Rev. Lett. 29, 597 (1972).
[22] M. I. Kaganov, I. M. Lifshitz, and L. V. Tanatarov, Zh. Eksp. Teor. Fiz. 31, 232 (1956) [Sov. Phys. JETP 4, 173 (1957)].

Translated by J. G. Adashko